

# Photoemission and high-order harmonic generation from solid surfaces in intense laser fields

F. H. M. Faisal,<sup>1</sup> J. Z. Kamiński,<sup>1,2</sup> and E. Saczuk<sup>2</sup>

<sup>1</sup>*Fakultät für Physik, Universität Bielefeld, 33615 Bielefeld, Germany*

<sup>2</sup>*Institute of Theoretical Physics, Warsaw University, Hoża 69, 00-681 Warszawa, Poland*

(Received 26 February 2005; published 16 August 2005)

We give a Floquet analysis of photoemission of electrons and high-order harmonic generation from a solid surface interacting with intense laser fields. A general theoretical algorithm, within a three-dimensional quasi-free-electron model, is presented. It takes account of the effective masses of the electron both within and outside the solid, as well as treating both reflected and refracted laser fields. The steady-state photocurrent is obtained from the diagonal photon components of the expectation value of the time-dependent current operator outside the surface, while the off-diagonal terms of the expectation value of the current operator from both inside and outside the surface provide the probability of coherent emission of high-order harmonic radiation. It is found, among other things, that electrons can be emitted from the surface requiring no net absorption of photons or even accompanied by emission of extra photons. The origin of the effect lies in the difference in the ponderomotive energy inside and outside the surface that can arise from the small ratio of the effective mass of the electron inside the solid (e.g., GaAs) and the mass of the free electron. Another result of qualitative significance is the formation of a plateau, well known in the atomic case, in both the kinetic energy distribution of the photocurrent and the spectrum of the high-order harmonic radiation. They are shown to arise in the present case from the evanescent part of the electron wave function at the surface.

DOI: [10.1103/PhysRevA.72.023412](https://doi.org/10.1103/PhysRevA.72.023412)

PACS number(s): 32.80.Wr, 42.65.Ky, 79.70.+q

## I. INTRODUCTION

Interaction of strong laser fields with solids and solid surfaces has been investigated for many years, both experimentally [1–13] and theoretically [14–28]. Since the system, in general, is very complex, many elementary processes overlap. This overlap creates difficulties in providing a clear physical interpretation of the results. Even theoretical investigations, which deal with simplified models, are not free from these problems entirely. They can, nevertheless, provide hints to the kind of elementary processes that dominate or become important for such complex systems. In the past much attention was focused on the role of intraband resonant transitions in solids and on how they influence the photocurrent energy distribution or the high-order harmonic spectrum (see, e.g., Refs. [21,23,11,12]). The aim of this paper is to discuss photoemission and high-order harmonic generation from a solid surface in an intense laser field, focusing our attention only on the surface effects. For this reason we shall adopt a three-dimensional quasi-free-electron model. This approximation will allow us to eliminate intraband resonance processes [23] and to investigate effects that are due solely to the presence of the surface. A general scheme of these phenomena is presented in Fig. 1. The incident, reflected, and refracted laser beams are assumed to be periodic functions of time, with the fundamental frequency  $\omega$ , which can have arbitrary higher-order harmonics. Thus, both monochromatic as well as harmonic pulses can be treated by the method. The polarization vectors of the beams are considered to be arbitrary and in principle uncorrelated, which allows one to incorporate possible changes of the reflected and refracted beams, as desired.

As mentioned above, the quasi-free-electron model does not account for intraband resonance transitions. Our earlier investigations of a one-dimensional model [23] suggest,

however, that these resonance transitions show up as sharp peaks in the photocurrent spectrum. We presume therefore that the model considered here should qualitatively describe well the average behavior of photoemission from a metal surface. Moreover, for slowly varying amplitude of the laser field, it should correctly account for multiphoton processes and interface transitions in semiconductor heterostructures with a space-dependent effective mass. In this sense our investigations complement theoretical models for ultrafast phenomena reviewed recently by Rossi and Kuhn [29].

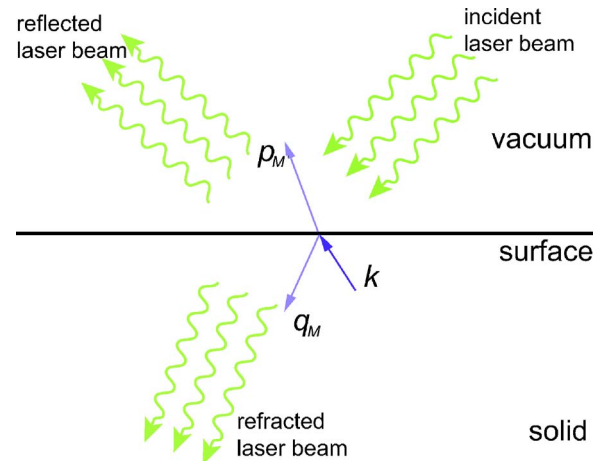


FIG. 1. (Color online) The laser beam of fundamental frequency  $\omega$  and intensity  $I$  is reflected and refracted by the surface with intensities  $\eta I$  and  $(1-\eta)I$ ,  $0 \leq \eta \leq 1$ . In the laser focus a crystal electron of momentum  $k$  is scattered by the surface and after absorption ( $M < 0$ ) or emission ( $M > 0$ ) of energy  $M\omega$  is transmitted or reflected with momentum  $p_M$  or  $q_M$ , respectively. During the collision of electrons with the surface higher-order harmonics of the fundamental frequency  $\omega$  are emitted.

The plan of this paper is the following. In the next section we present a quasi-free-electron model of the solid surface that accounts for the different effective masses of the electrons inside and outside, and allows for the modification of the reflected and refracted laser beams due to the presence of the surface. This model is applied in Sec. III to investigate photoemission, where the energy distribution of the laser-field-induced photoelectron current is calculated. A phenomenon that may be called a “ponderomotive ionization” effect, which can occur without the absorption of a laser photon or even with the emission of extra photons, is predicted. Section IV analyzes the appearance of a *plateau* in the energy distribution of the high-order harmonics. The paper ends with the conclusions and prospects in Sec. V. In this paper, Hartree atomic units (a.u.) ( $|e|=\hbar=m=1, c=1/\alpha$ ) are used, unless stated explicitly otherwise.

## II. QUASI-FREE-ELECTRON MODEL

In the following we shall assume that electrons in solids move freely, but with an effective mass  $m^*$  that is in general different from their rest mass  $m$  in vacuum. The solid surface is described by a step potential. To be more specific, the dynamics of electrons is assumed to be governed by the following Schrödinger equation:

$$i\partial_t\psi_V = \left[ \frac{1}{2} \left( \frac{1}{i} \nabla + \frac{1}{c} \mathbf{A}(t) \right)^2 \right] \psi_V, \quad z > 0,$$

$$i\partial_t\psi_C = \left[ \frac{1}{2m^*} \left( \frac{1}{i} \nabla + \frac{1}{c} \mathbf{A}_C(t) \right)^2 + V_S \right] \psi_C, \quad z < 0. \quad (1)$$

The surface is defined by the equation  $z=0$ . In the wave equation above,  $\mathbf{A}(t)$  and  $\mathbf{A}_C(t)$  are the vector potentials of the radiation fields in the vacuum and in the solid, respectively. The constant  $V_S = -(E_F + W)$  determines the surface potential with  $E_F$  being the Fermi energy and  $W$  being the work function. We shall apply the dipole approximation to the radiation field and assume that the vector potentials are periodic functions of time, i.e.,

$$\mathbf{A}(t) = \sum_{N_L=-N_0}^{N_0} e^{-iN_L\omega t} \mathbf{a}_{N_L}, \quad (2)$$

$$\mathbf{A}_C(t) = \sum_{N_L=-N_0}^{N_0} e^{-iN_L\omega t} \mathbf{a}_{C,N_L}, \quad (3)$$

where  $\mathbf{a}_{N_L}$  and  $\mathbf{a}_{C,N_L}$  are arbitrary complex (constant) vectors and  $N_0$  is the maximum harmonic order of the incident laser field. For  $N_0=1$ , for example, we have a typical laser field with a single carrier frequency. In the following we shall treat the constant vectors as phenomenological parameters of our theory. This is because adsorbed atoms or molecules generally have a significant influence on the electronic structure of the surface, which leads to strong modifications of work functions [30–32], and of the optical properties of the surface (see, e.g., Ref. [28]), which may be modeled by suitably changing the constants.

The conservation of probability implies that the wave functions  $\psi_V(\mathbf{r}, t)$  and  $\psi_C(\mathbf{r}, t)$  must satisfy the continuity conditions at the surface (for the one-dimensional case see, e.g., Refs. [22,33–37]),

$$\psi_V(\mathbf{r}, t)|_{z=0} = \psi_C(\mathbf{r}, t)|_{z=0}, \quad (4)$$

$$\mathbf{n}_S \cdot \left( \frac{1}{i} \nabla + \frac{1}{c} \mathbf{A}(t) \right) \psi_V(\mathbf{r}, t) \Big|_{z=0} = \frac{1}{m^*} \mathbf{n}_S \cdot \left( \frac{1}{i} \nabla + \frac{1}{c} \mathbf{A}_C(t) \right) \psi_C(\mathbf{r}, t) \Big|_{z=0}, \quad (5)$$

valid for all times  $t$ . In the equation above  $\mathbf{n}_S$  means the unit vector normal to the surface. Due to the time periodicity of the radiation field these wave functions can be Fourier decomposed:

$$\psi_V(\mathbf{r}, t) = e^{-iEt} \sum_{N \in \mathbb{Z}} e^{-iN\omega t} \psi_{V,N}(\mathbf{r}), \quad (6)$$

$$\psi_C(\mathbf{r}, t) = e^{-iEt} \sum_{N \in \mathbb{Z}} e^{-iN\omega t} \psi_{C,N}(\mathbf{r}), \quad (7)$$

with the same quasienergy  $E$ .  $\mathbb{Z}$  stands for the set of all integers. The explicit forms of  $\psi_{V,N}(\mathbf{r})$  and  $\psi_{C,N}(\mathbf{r})$  are determined by the Schrödinger equation, surface matching conditions, and the boundary conditions relevant for the process we are considering.

## III. PHOTOEMISSION

### A. Theory

First, let us consider a process that consists in the reflection by and the transmission through the surface of an incident electron of momentum  $\mathbf{k}$ . Without the laser field, solutions of the Schrödinger equation adopt the form

$$\psi_V(\mathbf{r}, t) = T_0 e^{-iEt + i\mathbf{p}_\parallel \cdot \mathbf{r}_\parallel - \kappa z}, \quad (8)$$

$$\psi_C(\mathbf{r}, t) = e^{-iEt} (e^{i\mathbf{k} \cdot \mathbf{r}} + R_0 e^{i\mathbf{k}_\parallel \cdot \mathbf{r}_\parallel - i\kappa z}), \quad (9)$$

in which  $\mathbf{p}_\parallel$ ,  $\kappa$ , and the transmission and reflection probability amplitudes  $T_0$  and  $R_0$  are determined from the matching conditions, Eqs. (4) and (5) (the symbol  $\parallel$  means parallel to the surface). In the presence of the laser field the wave function has a similar form, which we write as

$$\psi_V(\mathbf{r}, t) = \psi_T(\mathbf{r}, t), \quad (10)$$

$$\psi_C(\mathbf{r}, t) = \psi_I(\mathbf{r}, t) + \psi_R(\mathbf{r}, t). \quad (11)$$

In the equations above the incident wave  $\psi_I(\mathbf{r}, t) = \psi_{\mathbf{k}}(\mathbf{r}, t)$  is the Volkov wave function of momentum  $\mathbf{k}$  in the solid with  $k_z > 0$ , whereas  $\psi_R(\mathbf{r}, t)$  and  $\psi_T(\mathbf{r}, t)$  describe the reflected and the transmitted waves, respectively. This means that  $\psi_R(\mathbf{r}, t)$  is composed of momenta with negative  $z$  components, and  $\psi_T(\mathbf{r}, t)$  contains waves of positive  $z$  components of momenta.

The Volkov wave function  $\psi_{\mathbf{k}}(\mathbf{r}, t)$  is known in the explicit form

$$\psi_{\mathbf{k}}(\mathbf{r}, t) = \exp \left[ i\mathbf{k} \cdot \mathbf{r} - i \int_0^t d\tau E_C \left( \mathbf{k} + \frac{1}{c} \mathbf{A}_C(\tau) \right) \right], \quad (12)$$

where

$$E_C(\mathbf{k}) = \frac{1}{2m^*} \mathbf{k}^2 + V_S, \quad (13)$$

and the quasienergy is equal to

$$E = \frac{1}{2m^*} \mathbf{k}^2 + V_S + U_C. \quad (14)$$

The last term in the above equation is the ponderomotive energy in the solid,

$$U_C = \frac{1}{2m^* c^2} \frac{\omega}{2\pi} \int_0^{2\pi/\omega} d\tau A_C^2(\tau). \quad (15)$$

As we see, Eq. (14) determines only the amplitude of the momentum  $\mathbf{k}$  for a given quasienergy  $E$ ,

$$|\mathbf{k}| = \sqrt{2m^*(E - V_S - U_C)}. \quad (16)$$

Hence, the Volkov solution can be written in an equivalent form,

$$\begin{aligned} \psi_{E,n}(\mathbf{r}) = \exp \left[ -iEt - i \int_0^t d\tau \left( \frac{1}{2m^* c^2} A_C^2(\tau) - U_C \right) \right. \\ \left. + i\sqrt{2m^*(E - V_S - U_C)} \cdot \left( \mathbf{r} - \frac{1}{m^* c} \int_0^t d\tau A_C(\tau) \right) \right], \end{aligned} \quad (17)$$

labeled now by the quasienergy  $E$  and the unit vector  $\mathbf{n}$ ,  $|\mathbf{n}|=1$ , which determines the direction of  $\mathbf{k}$ . This form of the Volkov solution is helpful in constructing the most general expressions for the reflected and transmitted waves,  $\psi_{\mathbf{R}}(\mathbf{r}, t)$  and  $\psi_{\mathbf{T}}(\mathbf{r}, t)$ .

During the process of reflection by and transmission through the surface an electron can not only absorb or emit energy  $M\omega$  with an arbitrary integer  $M$ , but also change its direction of propagation. This leads to reflected and transmitted waves at any time  $t$  of the form

$$\begin{aligned} \psi_{\mathbf{R}}(\mathbf{r}, t) = \sum_{M \in \mathbb{Z}} R_M \exp \left[ -i(E + M\omega)t + i\mathbf{q}_M \cdot \mathbf{r} \right. \\ \left. - i \int_0^t d\tau \left( \frac{1}{m^* c} \mathbf{q}_M \cdot \mathbf{A}_C(\tau) + \frac{1}{2m^* c^2} A_C^2(\tau) - U_C \right) \right] \end{aligned} \quad (18)$$

and

$$\begin{aligned} \psi_{\mathbf{T}}(\mathbf{r}, t) = \sum_{M \in \mathbb{Z}} T_M \exp \left[ -i(E + M\omega)t + i\mathbf{p}_M \cdot \mathbf{r} \right. \\ \left. - i \int_0^t d\tau \left( \frac{1}{c} \mathbf{p}_M \cdot \mathbf{A}(\tau) + \frac{1}{2c^2} A^2(\tau) - U_V \right) \right]. \end{aligned} \quad (19)$$

The matching conditions (4) and (5), which have to be sat-

isfied for arbitrary  $x$  and  $y$  on the surface  $z=0$ , require that all momenta  $\mathbf{p}_{M\parallel}$  and  $\mathbf{q}_{M\parallel}$  parallel to the surface are equal,

$$\mathbf{p}_{M\parallel} = \mathbf{q}_{M\parallel} = \mathbf{k}_{\parallel}. \quad (20)$$

For momenta perpendicular to the surface we have

$$p_{M,z}^2 = 2(E + M\omega - U_V) - \mathbf{k}_{\parallel}^2, \quad (21)$$

$$q_{M,z}^2 = 2m^*(E + M\omega - V_S - U_C) - \mathbf{k}_{\parallel}^2. \quad (22)$$

The channels for which  $p_{M,z}^2 > 0$  are called open channels, as opposed to the so-called closed channels, for which  $p_{M,z}^2 \leq 0$ , and similarly for reflected waves. Taking the square root of the equations above we have to account for the boundary conditions and the normalizability of the wave function. The proper choice is the following:

$$p_{M,z} = \begin{cases} \sqrt{p_{M,z}^2} & \text{for open channels,} \\ i\sqrt{|p_{M,z}^2|} & \text{for closed channels,} \end{cases} \quad (23)$$

and

$$q_{M,z} = \begin{cases} -\sqrt{q_{M,z}^2} & \text{for open channels,} \\ -i\sqrt{|q_{M,z}^2|} & \text{for closed channels.} \end{cases} \quad (24)$$

Next we Fourier-analyze the functions periodic in time [see Eqs. (18) and (19)],

$$\begin{aligned} \exp \left[ -i\mathbf{k} \cdot \int_0^t d\tau \frac{1}{m^* c} \mathbf{A}_C(\tau) - i \int_0^t d\tau \left( \frac{1}{2m^* c^2} A_C^2(\tau) - U_C \right) \right] \\ = \sum_{N \in \mathbb{Z}} e^{-iN\omega t} C_N, \end{aligned} \quad (25)$$

$$\begin{aligned} \exp \left[ -i\mathbf{q}_M \cdot \int_0^t d\tau \frac{1}{m^* c} \mathbf{A}_C(\tau) - i \int_0^t d\tau \left( \frac{1}{2m^* c^2} A_C^2(\tau) - U_C \right) \right] \\ = \sum_{N \in \mathbb{Z}} e^{-iN\omega t} C_{N,M}, \end{aligned} \quad (26)$$

and

$$\begin{aligned} \exp \left[ -i\mathbf{p}_M \cdot \int_0^t d\tau \frac{1}{c} \mathbf{A}(\tau) - i \int_0^t d\tau \left( \frac{1}{2c^2} A^2(\tau) - U_V \right) \right] \\ = \sum_{N \in \mathbb{Z}} e^{-iN\omega t} V_{N,M}. \end{aligned} \quad (27)$$

This leads to the solution, which is suitable for our further discussion,

$$\begin{aligned} \psi_C(\mathbf{r}, t) = \sum_{M \in \mathbb{Z}} e^{-i(E+M\omega)t} e^{i\mathbf{k} \cdot \mathbf{r}} C_M \\ + \sum_{M,N \in \mathbb{Z}} R_N e^{-i(E+M\omega)t} e^{i\mathbf{q}_N \cdot \mathbf{r}} C_{M-N,N}, \end{aligned} \quad (28)$$

$$\psi_V(\mathbf{r}, t) = \sum_{M,N \in \mathbb{Z}} T_N e^{-i(E+M\omega)t} e^{i\mathbf{p}_N \cdot \mathbf{r}} V_{M-N,N}. \quad (29)$$

Let us note in passing that the coefficients  $C_M$ ,  $C_{M,N}$ , and  $V_{M,N}$  satisfy the important summation rules for open channels,

$$\sum_{M' \in Z} C_{M+M'} C_{M'}^* = \delta_{M,0}, \quad (30)$$

$$\sum_{M' \in Z} C_{M+M',N} C_{M',N}^* = \delta_{M,0}, \quad (31)$$

$$\sum_{M' \in Z} V_{M+M',N} V_{M',N}^* = \delta_{M,0}, \quad (32)$$

which are used as a check for numerical calculations. In practice they are computed by the fast Fourier transform of the periodic part of the wave functions Eqs. (12), (18), and (19). The reflection and transmission amplitudes  $R_N$  and  $T_N$  are still to be determined by applying the matching conditions, i.e., Eqs. (4) and (5). This leads to the following system of linear equations for  $R_N$  and  $T_N$ :

$$C_M + \sum_{N \in Z} C_{M-N,N} R_N = \sum_{N \in Z} V_{M-N,N} T_N, \quad (33)$$

$$\begin{aligned} & \sum_{N_L=-N_0}^{N_0} \frac{1}{m^*} \mathbf{n}_S \cdot \left( \mathbf{k} \delta_{N_L,0} + \frac{1}{c} \mathbf{a}_{C,N_L} \right) C_{M-N_L} \\ & + \sum_{N \in Z} \left[ \sum_{N_L=-N_0}^{N_0} \frac{1}{m^*} \mathbf{n}_S \cdot \left( \mathbf{q}_N \delta_{N_L,0} + \frac{1}{c} \mathbf{a}_{C,N_L} \right) C_{M-N_L-N,N} \right] R_N \\ & = \sum_{N \in Z} \left[ \sum_{N_L=-N_0}^{N_0} \mathbf{n}_S \cdot \left( \mathbf{p}_N \delta_{N_L,0} + \frac{1}{c} \mathbf{a}_{N_L} \right) V_{M-N_L-N,N} \right] T_N, \end{aligned} \quad (34)$$

which can be solved numerically by truncating the domain of the Fourier indices to a finite set. Such a truncation, however, has to be done carefully. Due to the conservation of probability the amplitudes  $R_N$  and  $T_N$  satisfy the unitary condition

$$\sum_N \prime \frac{q_{N,z}}{k_z} |R_N|^2 + \sum_N \prime \frac{m^* p_{N,z}}{k_z} |T_N|^2 = 1, \quad (35)$$

in which the prime over the sum symbol means summation only over the open channels. It may happen that if the truncation is too drastic, we shall not be able to satisfy this equation with a sufficient precision. In order to achieve this goal for higher laser-field intensities, we had to perform the calculations in quadruple precision.

Having calculated the amplitudes  $R_N$  and  $T_N$  we can determine the cycle-averaged electric current of photoelectrons by evaluating the expectation value of the probability current in the vacuum,

$$\left\langle \text{Re} \left[ \psi_T^* \left( \frac{1}{i} \nabla + \frac{1}{c} \mathbf{A} \right) \psi_T \right] \right\rangle = \sum_N \prime \mathbf{p}_N |T_N|^2, \quad (36)$$

where we sum over the open channels. Further we have to sum over all occupied states of electrons in the crystal with  $k_z \geq 0$ , which leads to the total current emitted by a unit surface

$$\mathbf{j} = - \frac{2}{(2\pi)^3} \int_{|k| \leq k_F, k_z > 0} d^3 k \sum_N \prime \mathbf{p}_N |T_N|^2. \quad (37)$$

Since  $T_N$  is the probability amplitude for electrons to be ionized from the surface with kinetic energy  $E_{\text{kin}} = \mathbf{p}_N^2 / 2 = \mathbf{k}^2 / 2m^* + V_S + U_C - U_V + N\omega$ , therefore we can write

$$\sum_N \prime \mathbf{p}_N |T_N|^2 = \int_0^\infty dE_{\text{kin}} \mathbf{P}(E_{\text{kin}}, \mathbf{k}), \quad (38)$$

with

$$\mathbf{P}(E_{\text{kin}}, \mathbf{k}) = \sum_N \prime \mathbf{p}_N |T_N|^2 \delta \left( \frac{\mathbf{k}^2}{2m^*} + V_S + U_C - U_V + N\omega - E_{\text{kin}} \right). \quad (39)$$

This permits us to define the energy distribution of photocurrent  $\mathcal{S}(E_{\text{kin}})$  per unit surface,

$$\mathbf{j} = \int_0^\infty dE_{\text{kin}} \mathcal{S}(E_{\text{kin}}), \quad (40)$$

with

$$\mathcal{S}(E_{\text{kin}}) = - \frac{2}{(2\pi)^3} \int_{|k| \leq k_F, k_z > 0} d^3 k \mathbf{P}(E_{\text{kin}}, \mathbf{k}). \quad (41)$$

Thus, the photocurrent energy distribution  $\mathcal{S}(E_{\text{kin}})$  is given as the three-dimensional integral over momenta  $\mathbf{k}$ , the integrand of which is evaluated by solving a system of linear equations for the transmission and reflection probability amplitudes.

## B. Photoionization current from sodium surface

We shall apply our theory to the sodium surface ( $z=0$ ), for in this metal the electrons may be assumed to move “freely”, with the effective mass close to the free-electron mass [38]. The work function and the Fermi energy for sodium metal are equal to 2.75 and 3.3 eV [38,39], respectively. For the incident laser beam we choose the monochromatic Ti:sapphire laser beam of frequency  $\omega = 1.5498\text{eV}$  ( $\lambda = 800\text{ nm}$ ) and with the linear polarization vector lying in the  $xz$  plane. Denoting by  $\theta_L$  the angle between the laser beam propagation direction and the normal ( $z$  axis) to the surface, we assume the case of specular reflection without penetration into the solid and write the electromagnetic vector potentials as

$$\begin{aligned} \mathbf{A}(t) &= \mathbf{e}_x \frac{c\sqrt{I}}{\omega} \cos \theta_L [-\sin(\omega t) + \sin(\omega t + \phi_R)] \\ &+ \mathbf{e}_z \frac{c\sqrt{I}}{\omega} \sin \theta_L [\sin(\omega t) + \sin(\omega t + \phi_R)], \\ \mathbf{A}_C(t) &= \mathbf{0}, \end{aligned} \quad (42)$$

where  $I$  and  $\omega$  are the incident beam intensity and frequency in atomic units. We shall investigate below the dependence of the photocurrent energy distribution, Eq. (41), on the change of phase  $\phi_R$  of the reflected beam. Other possible

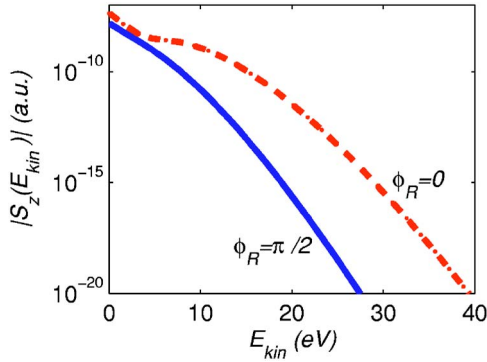


FIG. 2. (Color online) Energy distribution of photocurrent perpendicular to the sodium surface per unit area [see Eq. (41)], for  $\theta_L = \pi/4$ ,  $\phi_R = \pi/2$  and 0. The vector potentials are defined by Eqs. (42) with the incident laser intensity and frequency equal to  $10^{13}$  W/cm $^2$  and 1.5498 eV. Note a strong dependence of the photocurrent on  $\phi_R$ .

modifications of the reflected and refracted beams, e.g., polarization characteristics of reflected light, could be accounted for if and when needed.

In Figs. 2 and 3 we show the normal component of the photocurrent energy distribution, Eq. (41), for the laser frequency  $\omega = 1.5498$  eV and for two incident intensities  $10^{13}$  and  $2 \times 10^{13}$  W/cm $^2$ . We observe a strong dependence of the probability of photocurrent on the angle  $\phi_R$ . This is consistent with the expectation that after ionization the electrons are accelerated by the laser field in the vacuum and gain energy proportional to the laser-field intensity. Indeed, for  $\phi_R = 0$  the electric-field strength of the combined incident and reflected beams is the maximum.

We attribute the existence of the dips and the formation of the plateaus in the spectrum to the rescattering effect [40–42] of photoelectrons by the surface potential. Such a rescattering is especially strong for  $\phi_R = 0$ . In this case the total electric field oscillates in the direction perpendicular to the surface with an amplitude  $2 \sin \theta_L = \sqrt{2}$  times larger than the amplitude for the incident laser beam. For  $\omega = 1.5498$  eV the intensity  $10^{13}$  W/cm $^2$  corresponds approximately to the pon-

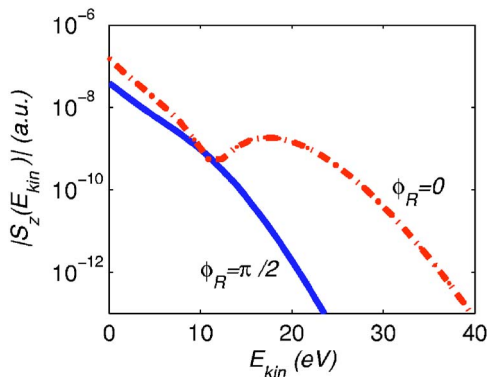


FIG. 3. (Color online) The same as in Fig. 2 but for the incident laser intensity  $2 \times 10^{13}$  W/cm $^2$ . Note that on doubling the incident intensity the photocurrent for larger energies increases by many orders of magnitude. For  $\phi_R = 0$  a plateau in the spectrum develops, which is analogous to the one observed in the atomic case.

deromotive energy in vacuum of 0.6 eV. Thus, the ponderomotive energy at the surface, for the incident intensity  $2 \times 10^{13}$  W/cm $^2$  and  $\phi_R = 0$ , equals  $U_V = 2.4$  eV. This shows that the maximum of the plateau in Fig. 3 should lie between  $7U_V$  and  $10U_V$ , which agrees quite well with what is observed in the atomic case [42]. An explanation for this agreement is that in this case the laser field interacts only with the evanescent part of the electron states, which is very similar to the bound-state wave function in the atomic case. We shall see below a similar effect on the emission of high-order harmonics.

The present investigations show that the enhanced high-energy part in the energy spectrum of photocurrent is due not only to the intraband resonant transitions in the crystal, as was pointed out in Refs. [23,11,12], but also to pure surface effects, as exemplified here. The sensitive dependence of the distributions on the properties of the surface (i.e., on the free parameters of our theory) such as  $\phi_R$  suggests that their knowledge in specific cases is essential for interpreting the experimental results.

### C. Ponderomotive ionization from a GaAs-like surface

Our next illustration shows a dramatic influence of effective mass on the photoeffect in intense laser fields. It is usually assumed that in ionization processes electrons need to absorb a minimum number of laser photons in order to pass into the continuum state. This, however, is not in general required to be true, as can be seen from the energy conservation  $\delta$  function in Eq. (39) and from the expressions for the ponderomotive energies  $U_C$  and  $U_V$ . If the effective mass of the electron is small compared to the rest mass of the electron in the vacuum, then the energy accumulated in the quiver motion of the electron in the laser field suffices for it to be ionized without net absorption of photons. Such ionizations may even occur along with the emission of *extra* laser photons. This can take place, for example, in the photoemission from gallium arsenide semiconductor surfaces, for in this material the effective mass  $m^*$  of the electron is a small fraction of its rest mass in vacuum,  $m^* = 0.0665$  (a.u.) [43]. Since in this case the Fermi level is just below the conduction band, we shall assume for the purpose of model calculations that  $E_F = 0$ , and  $W = 4$  eV (a value close to the work functions for Ga and As crystals [39]). For the incident laser frequency we take the third harmonic of the Ti:sapphire laser ( $\omega = 3 \times 0.056$  a.u.) and calculate the Fourier components of electric current densities of the conduction electrons that move perpendicularly to the surface, i.e.,  $k_x = k_y = 0$ , and  $k_z$  varies from zero to its maximum value  $k_{\max}$  for which  $E_C(k_{\max}) = 0$  (corresponding to the initially bound electrons). The electric current density associated with the absorption of  $N$  photons [see Eq. (36)] is

$$j_N(\mathbf{k}) = -\mathbf{p}_N |T_M|^2, \quad (43)$$

evaluated at  $\mathbf{k} = k_z \mathbf{e}_z$ .

In Fig. 4 we present the Fourier components of the current density for the laser intensity  $I = 10^{14}$  W/cm $^2$  and  $\theta_L = \pi/2$  (grazing incidence). For weak laser beams electrons have to absorb at least one laser photon in order to be emitted into

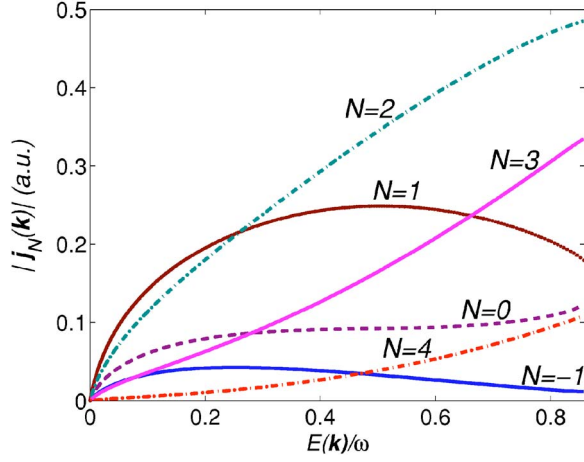


FIG. 4. (Color online) The transition current Eq. (43) as a function of electron kinetic energy  $E(\mathbf{k})=k^2/2m^*$  in the solid for  $k_x=k_y=0$ . The laser-field intensity and frequency of the incident laser beam are equal to  $10^{14}$  W/cm<sup>2</sup> and  $\omega=3 \times 1.5498$  eV,  $\eta=0$  (no reflected beam), and  $\theta_L=\pi/2$  (grazing incidence) [see Eq. (42)]. The laser beam is taken to be linearly polarized with the polarization vector perpendicular to the surface. For low intensities the absorption of at least one laser photon is needed for electron emission into the vacuum. For the high intensity considered here electrons can be emitted into the vacuum by absorption of no net number of photons or even by emitting one extra photon ( $N=-1$ ). Such a phenomenon can occur generally whenever a large difference between the ponderomotive energies in the solid and the vacuum exists.

the vacuum. This is also usually the case for strong laser fields if the effective mass of electrons in the crystal is not smaller than the rest mass. However for  $m^* \ll 1$  (e.g., GaAs) the pattern changes significantly since the large ponderomotive energy accumulated in the quiver motion of conduction electrons can be transferred, during the collision of the electrons with the surface, into longitudinal motion in the vacuum. The difference in the ponderomotive energies inside and outside the surface can be large enough for the bound electrons even to emit excess laser photons (by a stimulated inverse bremsstrahlung mechanism) and still become free.

#### IV. HIGH-ORDER HARMONIC GENERATION

##### A. Theory

To investigate the emission of coherent high-order harmonic radiation we need the Fourier decomposition of the expectation value of the probability current density operator. Let us first consider the vacuum part of the wave function given by Eq. (29). The current density in this case [cf. the left-hand side of Eq. (36)] can be written down, after some simple algebraic manipulations, as

$$\begin{aligned} j_V(\mathbf{r}, t) &= \sum_{M \in \mathbb{Z}} e^{-iM\omega t} \sum_{N, N' \in \mathbb{Z}} e^{i(p_N - p_{N'}) \cdot \mathbf{r}} T_N T_{N'}^* \\ &\times \sum_{N_L = -N_0}^{N_0} \left( \frac{\mathbf{p}_N + \mathbf{p}_{N'}}{2} \delta_{N_L, 0} + \frac{1}{c} \mathbf{a}_{N_L} \right) \\ &\times \sum_{M' \in \mathbb{Z}} V_{M+M'-N_L-N, N} V_{M'-N', N'}^*. \end{aligned} \quad (44)$$

Since we are interested in the scattered radiation with harmonic modes other than the incident modes, therefore all terms with  $N=N'$  (for open channels) can be excluded from the sum above. Hence, the expectation value of the probability current density contributing to the high-order harmonics of interest is equal to

$$\begin{aligned} J_V(t) &= S \sum_{M > N_0} e^{-iM\omega t} \sum_{\substack{N, N' \in \mathbb{Z} \\ N \neq N'}} \frac{T_N T_{N'}^*}{-i(p_N - p_{N'})_z} \\ &\times \sum_{N_L = -N_0}^{N_0} \left( \frac{\mathbf{p}_N + \mathbf{p}_{N'}}{2} \delta_{N_L, 0} + \frac{1}{c} \mathbf{a}_{N_L} \right) \\ &\times \sum_{M' \in \mathbb{Z}} V_{M+M'-N_L-N, N} V_{M'-N', N'}^*, \end{aligned} \quad (45)$$

where  $\neq$  over the sum symbol excludes  $N=N'$  for open channels and  $S$  is the total area of the surface on which the laser beam shines. Analogously, one can calculate the contribution coming from the reflected and the incident parts of the wave function inside the solid, Eq. (28). Combining all of them together we arrive at the total expectation value of the probability current for an electron state characterized by the initial momentum  $\mathbf{k}$ ,

$$\mathbf{J}(\mathbf{k}, t) = S \sum_{M > N_0} e^{-iM\omega t} \mathbf{J}_M(\mathbf{k}), \quad (46)$$

with

$$\mathbf{J}_M(\mathbf{k}) = \mathbf{J}_{V, M}(\mathbf{k}) + \mathbf{J}_{R, M}(\mathbf{k}) + \mathbf{J}_{ir, M}(\mathbf{k}), \quad (47)$$

where

$$\begin{aligned} \mathbf{J}_{V, M}(\mathbf{k}) &= \sum_{\substack{N, N' \in \mathbb{Z} \\ N \neq N'}} \frac{T_N T_{N'}^*}{-i(p_N - p_{N'})_z} \sum_{N_L = -N_0}^{N_0} \left( \frac{\mathbf{p}_N + \mathbf{p}_{N'}}{2} \delta_{N_L, 0} \right. \\ &\left. + \frac{1}{c} \mathbf{a}_{N_L} \right) \sum_{M' \in \mathbb{Z}} V_{M+M'-N_L-N, N} V_{M'-N', N'}^*, \end{aligned} \quad (48)$$

$$\begin{aligned} \mathbf{J}_{R, M}(\mathbf{k}) &= \sum_{\substack{N, N' \in \mathbb{Z} \\ N \neq N'}} \frac{R_N R_{N'}^*}{i(q_N - q_{N'})_z} \sum_{N_L = -N_0}^{N_0} \frac{1}{m^*} \left( \frac{\mathbf{q}_N + \mathbf{q}_{N'}}{2} \delta_{N_L, 0} \right. \\ &\left. + \frac{1}{c} \mathbf{a}_{C, N_L} \right) \sum_{M' \in \mathbb{Z}} C_{M+M'-N_L-N, N} C_{M'-N', N'}^*, \end{aligned} \quad (49)$$

and

$$\begin{aligned} \mathbf{J}_{ir, M}(\mathbf{k}) &= \sum_{N \in \mathbb{Z}} \frac{R_N}{i(q_N - k)_z} \sum_{N_L = -N_0}^{N_0} \frac{1}{m^*} \left( \frac{\mathbf{q}_N + \mathbf{k}}{2} \delta_{N_L, 0} \right. \\ &\left. + \frac{1}{c} \mathbf{a}_{C, N_L} \right) \sum_{M' \in \mathbb{Z}} C_{M+M'-N_L-N, N} C_{M'}^* \\ &- \sum_{N \in \mathbb{Z}} \frac{R_N^*}{i(q_N^* - k)_z} \sum_{N_L = -N_0}^{N_0} \frac{1}{m^*} \left( \frac{\mathbf{q}_N^* + \mathbf{k}}{2} \delta_{N_L, 0} \right. \end{aligned}$$

$$+ \frac{1}{c} \mathbf{a}_{C,N_L} \Big) \sum_{M' \in \mathbb{Z}} C_{-M+M'-N_L-N,N}^* C_{M'} \quad (50)$$

In the equations above the Fourier components  $J_{V,M}(\mathbf{k})$  arise from  $\langle \psi_T(t) | \hat{\mathbf{p}} + \mathbf{A}(t)/c | \psi_T(t) \rangle$  (vacuum current),  $J_{R,M}(\mathbf{k})$  from  $\langle \psi_R(t) | \hat{\mathbf{p}} + \mathbf{A}_C(t)/c | \psi_R(t) \rangle / m^*$  (reflected current), and  $J_{I,M}(\mathbf{k})$  from  $\langle \psi_I(t) | \hat{\mathbf{p}} + \mathbf{A}_C(t)/c | \psi_R(t) \rangle / m^* + c.c.$  (interference current), where  $\hat{\mathbf{p}}$  is the momentum operator.

The cycle-averaged power of the  $M$ th-order harmonic radiated by an electron of incident momentum  $\mathbf{k}$  in the solid angle  $d\Omega$  and in the direction of a unit vector  $\mathbf{n}$  is equal to [44]

$$\frac{dP_M(\mathbf{k})}{d\Omega} = \frac{M^2 \omega^2 S^2}{8\pi c^3} \{ \mathbf{J}_M(\mathbf{k}) \cdot \mathbf{J}_M^*(\mathbf{k}) - [\mathbf{n} \cdot \mathbf{J}_M(\mathbf{k})][\mathbf{n} \cdot \mathbf{J}_M^*(\mathbf{k})] \}, \quad (51)$$

and the angle-integrated power emitted is

$$P_M(\mathbf{k}) = \frac{M^2 \omega^2 S^2}{3c^3} [\mathbf{J}_M(\mathbf{k}) \cdot \mathbf{J}_M^*(\mathbf{k})]. \quad (52)$$

Next, in order to determine the power emitted by the high-order harmonics we sum the contributions from all the occupied states of electrons in the solid. Thus we obtain the differential power spectrum of the  $M$ th-order harmonic

$$\frac{dP_M}{d\Omega} = \frac{M^2 \omega^2 S^2}{2(2\pi)^4 c^3} \int_{|k| \leq k_F, k_z > 0} d^3k [|\mathbf{J}_M(\mathbf{k})|^2 - |\mathbf{n} \cdot \mathbf{J}_M(\mathbf{k})|^2], \quad (53)$$

and the angle-integrated power

$$P_M = \frac{2M^2 \omega^2 S^2}{3(2\pi)^3 c^3} \int_{|k| \leq k_F, k_z > 0} d^3k |\mathbf{J}_M(\mathbf{k})|^2. \quad (54)$$

### B. Harmonic generation from sodium surface

In this subsection we present the high-order harmonic spectra for the laser-field configuration described by Eq. (42), and only for the lower intensity  $10^{13}$  W/cm<sup>2</sup> (for higher intensities the computation time becomes too long). We shall also confine our discussion to the case of the phase shift in reflection  $\phi_R = \pi/2$ . In Fig. 5 we present the total power spectrum of high-order harmonics. We observe the existence of a plateau in the high-order harmonic spectrum. It ends at  $M_{\text{cutoff}} = 5$ , which matches quite well with the cutoff formula

$$E_F + W + 3U_V = M_{\text{cutoff}} \omega. \quad (55)$$

This is a generalization of the formula  $I + 3U_p \approx M_{\text{cutoff}} \omega$  known in the atomic case [41] to the case of the surface where the reflection phase  $\phi_R = \pi/2$  and the direction of the beam with respect to the normal to the surface  $\theta_L = \pi/4$ . Note that in this case the vector potential in the vacuum is of the form

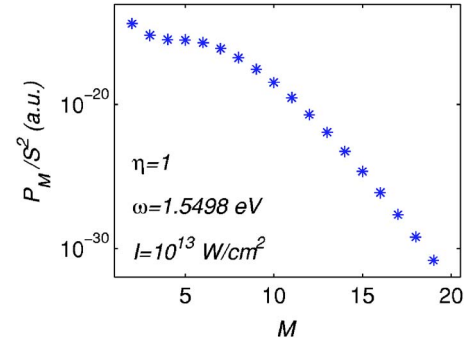


FIG. 5. (Color online) The angle-integrated high-order harmonic spectrum [in atomic units, computed from Eq. (54)]; laser intensity  $I = 10^{13}$  W/cm<sup>2</sup> and frequency  $\omega = 1.5498$  eV. The laser field is defined by Eq. (42). Note the appearance of a plateau with a cutoff estimated by the formula  $M_{\text{cutoff}} \omega \approx E_F + W + 3U_V$  for  $M_{\text{cutoff}} = 5$ . The plateau arises from the *evanescent* part of the wave function at the surface.

$$\mathbf{A}(t) = \frac{c\sqrt{I}}{\omega} \left[ \mathbf{e}_x \cos\left(\omega t + \frac{\pi}{4}\right) + \mathbf{e}_z \sin\left(\omega t + \frac{\pi}{4}\right) \right]. \quad (56)$$

Thus, the maximum electric field in the vacuum is equal to the maximum electric field of the incident laser beam and hence  $U_V = 0.6$  eV. This equality permits us to relate the high-order harmonic generation with the recombination process of photoelectrons to the evanescent part of the electron wave function in the vacuum during the rescattering process with the surface. Note that now all the conduction electrons take part in the harmonic generation from the plateau and not only those with energy close to the Fermi energy. It would be interesting to check the cutoff formula at higher intensities in the future.

The analysis of the differential power spectrum shows that high-order harmonics are radiated predominantly parallel to the surface and in the direction perpendicular to the plane of reflection of the laser field (which in our case is the  $xz$  plane). This is shown for the seventh-order harmonic in Fig. 6. For other values of  $M$  the pattern looks similar. It is interesting, however, to notice that for harmonics from the plateau the radiation in the  $xy$  plane is virtually isotropic, in contrast to the case of the other harmonics. The differential power spectrum in the  $xy$  plane is shown in Fig. 7 as a polar plot. It clearly differs from that observed for a differential power spectrum obtained for the high-order harmonics emitted from a gas jet, where the emission is predominantly in the direction of propagation of the incident laser beam. The pattern seen in the present case is consistent with the experimental observations of surface harmonics generated at relativistic laser-field intensities [5,9].

We may define the *efficiency* of high-order harmonic generation as the ratio of the total power of high-order harmonics to the total power of the incident laser beam. Let the laser spot on the surface be of the order of  $\lambda^2$ , where  $\lambda$  is the wavelength of the incident laser beam; then the efficiency for the generation of the  $M$ th-order harmonic,  $\mathcal{E}_M$ , is

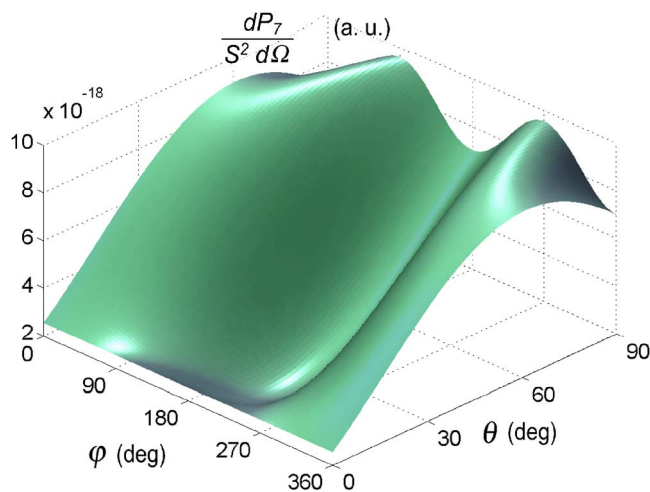


FIG. 6. (Color online) The differential power spectrum of the seventh-order harmonic for  $I=10^{13}$  W/cm<sup>2</sup>,  $\omega=1.5498$  eV,  $\theta_L=\pi/4$ , and  $\phi_R=\pi/2$ . The harmonics are radiated predominantly in the surface plane ( $\theta=\pi/2$ ) and in the directions perpendicular to the laser-field propagation ( $\varphi=\pi/2$  and  $3\pi/2$ ).

$$\mathcal{E}_M \equiv \frac{P_M}{I\lambda^2}. \quad (57)$$

For the fifth-order harmonic (the last harmonic from the plateau in Fig. 5) we find  $P_5=3\times 10^{-16}\lambda^4$  a.u. Since for the laser frequency  $\omega=1.5498$  eV the wavelength equals  $\lambda\approx 1.5\times 10^4$  a.u., for  $I=10^{13}$  W/cm<sup>2</sup> the efficiency  $\mathcal{E}_M\approx 10^{-4}$ , which is comparable to (or could be even higher than) the case of high-order harmonics generated in gas jets.

## V. CONCLUSIONS

In this paper we presented a three-dimensional theoretical scheme for the calculation of the photocurrent and high-order harmonic radiation emitted from a surface irradiated by a strong laser field. We have assumed a quasi-free-electron model with different effective masses inside and outside the surface. It allowed us to consider arbitrary forms of the incident, reflected, and refracted laser beams. Different characteristics of the reflected and refracted beams (e.g., different polarization vectors, relative phases, and intensities) are treated as phenomenological parameters, which could be chosen to model the different reflection or refraction properties of the surfaces of interest. Both the kinetic energy distribution of the photocurrent and the high-order harmonic spectrum are found to depend sensitively on the phenomenological parameters chosen. In particular, the high-energy part of the photocurrent is dependent strongly on the macroscopic (reflection, transmission, and refraction) characteristics of the beam at the surface. For the case of specular reflection of the incident laser beam (no significant penetration) both the kinetic energy distribution of the photocurrent and the high-

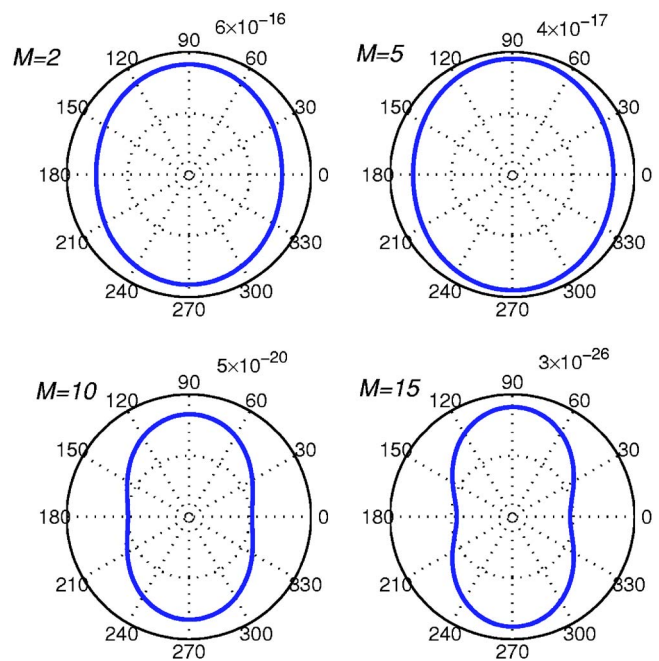


FIG. 7. (Color online) The polar plots of differential power spectra (in a.u.) for  $I=10^{13}$  W/cm<sup>2</sup>,  $\omega=1.5498$  eV,  $\theta_L=\pi/4$ ,  $\phi_R=\pi/2$ , and  $\theta=\pi/2$  (cf. Fig. 6). The harmonics from the plateau are almost isotropically distributed.

order harmonic spectrum exhibit plateaus, with properties similar to the ones observed in the atomic case. They arise in the present case from the evanescent part of the electron state at the surface. We also found a strong dependence of the photocurrent on the change of the electron's effective mass. In particular, the electrons can be emitted in the vacuum with no net absorption of photons or even along with the emission of extra photons. This phenomenon, which may be called a “ponderomotive ionization” effect, is due to the difference of ponderomotive energies of electrons in the solid and the vacuum, arising from the difference in the effective electron masses inside and outside the crystal. Finally, we may point out that the general theoretical scheme presented here can be used to model more complex physical situations than that considered here explicitly. For example, it would allow one to analyze photoemission and high-order harmonic generation by trains of attosecond pulses that are currently under active investigation.

## ACKNOWLEDGMENTS

It is a pleasure to thank Professor Hans Steidl for fruitful discussions about surface physics. J.Z.K. thanks Professor U. Heinzman and Dr. M. Drescher for their invitation as a visiting scientist at SFB 613. This work is partially supported by the DFG-Schwerpunktprojekt SPP1053 under Project No. FA160/18-3, and by the Polish Committee for Scientific Research Grant No. KBN 1 P03B 069 26.

- [1] Gy. Farkas, Cs. Tóth, S. D. Moustazis, N. A. Papadogiannis, and C. Fotakis, *Phys. Rev. A* **46**, R3605 (1992).
- [2] S. Kohlweyer, G. D. Tsakiris, C.-G. Wahlström, C. Tillman, and I. Marcer, *Opt. Commun.* **177**, 431 (1995).
- [3] D. von der Linde, T. Engers, G. Jenke, P. Agostini, G. Grillon, E. Nibbering, A. Mysyrowicz, and A. Antonetti, *Phys. Rev. A* **52**, R25 (1995).
- [4] B. C. Stuart, M. D. Feit, S. Herman, A. M. Rubenchik, B. W. Shore, and M. D. Perry, *Phys. Rev. B* **53**, 1749 (1996).
- [5] J. Zhang, M. Zepf, P. A. Norreys, A. E. Dangor, M. Bakarezos, C. N. Danson, A. Dyson, A. P. Fews, P. Gibbon, M. H. Key, P. Lee, P. Loukakos, S. Moustazis, D. Neely, F. N. Walsh, and J. S. Wark, *Phys. Rev. A* **54**, 1597 (1996).
- [6] A. Haché, Y. Kostoulas, R. Atanasov, J. L. P. Hughes, J. E. Sipe, and H. M. van Driel, *Phys. Rev. Lett.* **78**, 306 (1997).
- [7] Gy. Farkas, Cs. Tóth, A. Köhási-Kis, P. Agostini, G. Petite, P. Martin, J. M. Berset, and J. M. Ortega, *J. Phys. B* **31**, L461 (1998).
- [8] F. Pisani, J. L. Fabre, S. Guizard, P. Palianov, Ph. Martin, F. Glotin, and J. M. Ortega, *Phys. Rev. Lett.* **87**, 187403 (2001).
- [9] I. Watts, M. Zepf, E. L. Clark, M. Tatarakis, K. Krushelnick, A. E. Dangor, R. M. Allott, R. J. Clarke, D. Neely, and P. A. Norreys, *Phys. Rev. Lett.* **88**, 155001 (2002).
- [10] U. Teubner, G. Pretzler, Th. Schlegel, K. Eidmann, E. Förster, and K. Witte, *Phys. Rev. A* **67**, 013816 (2003).
- [11] A. Belsky, P. Martin, H. Bachau, A. N. Vasil'ev, B. N. Yatsenko, S. Guizard, G. Geoffroy, and G. Petite, *Europhys. Lett.* **67**, 301 (2004).
- [12] A. Belsky, H. Bachau, J. Gaudin, G. Geoffroy, S. Guizard, P. Martin, G. Petite, A. N. Vasil'ev, and B. N. Yatsenko, *Appl. Phys. B: Lasers Opt.* **78**, 989 (2004).
- [13] A. Srivastava, R. Srivastava, J. Wang, and J. Kono, *Phys. Rev. Lett.* **93**, 157401 (2004).
- [14] L. Plaja and L. Roso-Franco, *Phys. Rev. B* **45**, 8334 (1992).
- [15] A. Misra and J. I. Gersten, *Phys. Rev. B* **43**, 1883 (1991); **45**, 8665 (1992).
- [16] J. Z. Kamiński, *Acta Phys. Pol. A* **83**, 495 (1993).
- [17] R. Atanasov, A. Haché, J. L. P. Hughes, H. M. van Driel, and J. E. Sipe, *Phys. Rev. Lett.* **76**, 1703 (1996).
- [18] P. Gibbon, *Phys. Rev. Lett.* **76**, 50 (1996).
- [19] D. von der Linde and K. Rzażewski, *Appl. Phys. B: Lasers Opt.* **63**, 499 (1996).
- [20] R. Lichters, J. Meyer-ter-Vehn, and A. Pukhov, *Phys. Plasmas* **3**, 3425 (1996).
- [21] F. H. M. Faisal and J. Z. Kamiński, *Phys. Rev. A* **54**, R1769 (1996).
- [22] F. H. M. Faisal and J. Z. Kamiński, *Phys. Rev. A* **56**, 748 (1997).
- [23] F. H. M. Faisal and J. Z. Kamiński, *Phys. Rev. A* **58**, R19 (1998).
- [24] A. N. Vasil'ev, Y. Fang, and V. V. Mikhailin, *Phys. Rev. B* **60**, 5340 (1999).
- [25] Ph. Martin, S. Vivirito, and G. Petite, *J. Phys. B* **33**, 767 (2000).
- [26] A. K. Gupta, O. E. Alon, and N. Moiseyev, *Phys. Rev. B* **68**, 205101 (2003).
- [27] O. E. Alon, *Phys. Rev. B* **67**, 121103(R) (2003).
- [28] G. Raşeev and D. Bejan, *Surf. Sci.* **528**, 196 (2003); D. Bejan and G. Raşeev, *ibid.* **528**, 163 (2003), and references therein.
- [29] F. Rossi and T. Kuhn, *Rev. Mod. Phys.* **74**, 895 (2002).
- [30] W. Mönch, *Semiconductor Surfaces and Interfaces* (Springer, Berlin, 2001).
- [31] H. Lüth, *Solid Surfaces, Interfaces and Thin Films* (Springer, Berlin, 2001).
- [32] M. C. Desjonquères and D. Spanjaard, *Concepts in Surface Physics* (Springer, Berlin, 1998).
- [33] J. M. Levy-Leblond, *Eur. J. Phys.* **13**, 215 (1992); *Phys. Rev. A* **52**, 1845 (1995).
- [34] S. Varró and F. Ehlötzky, *J. Phys. B* **31**, 2145 (1998).
- [35] J. Z. Kamiński and F. Ehlötzky, *J. Phys. B* **32**, 3193 (1999).
- [36] N. Moiseyev and R. Lefebvre, *Phys. Rev. A* **64**, 052711 (2001).
- [37] E. Sączuk and J. Z. Kamiński, *Phys. Status Solidi B* **240**, 603 (2003).
- [38] U. Mizutani, *Introduction to the Electron Theory of Metals* (Cambridge University Press, Cambridge, U.K., 2001).
- [39] H. B. Michelson, *J. Appl. Phys.* **48**, 4729 (1977).
- [40] M. Y. Kuchiev, *JETP Lett.* **45**, 404 (1987).
- [41] J. L. Krause, K. J. Schafer, and K. C. Kulander, *Phys. Rev. Lett.* **68**, 3535 (1992); K. C. Kulander, K. J. Schafer, and J. L. Krause, in *Super-Intense Laser-Atom Physics*, edited by B. Piraux, A. L'Huillier, and K. Rzażewski (Plenum, New York, 1993), p. 95; P. B. Corkum, *Phys. Rev. Lett.* **71**, 1994 (1993).
- [42] W. Becker, A. Lohr, and M. Kleber, *Quantum Semiclass. Opt.* **7**, 423 (1995); W. Becker, F. Grasbon, R. Kopold, D. B. Milošević, G. G. Paulus, and H. Walther, *Adv. At., Mol., Opt. Phys.* **48**, 35 (2002).
- [43] R. Enderlein and N. J. M. Horing, *Fundamentals of Semiconductor Physics and Devices* (World Scientific, Singapore, 1997).
- [44] J. D. Jackson, *Classical Electrodynamics* (Wiley, New York, 1980).